ЖЭТФ, 2022, том 162, вып. 2 (8), стр. 177–180

THE CASIMIR EFFECT IN BOSE–EINSTEIN CONDENSATE MIXTURES CONFINED BY A PARALLEL PLATE GEOMETRY IN THE IMPROVED HARTREE–FOCK APPROXIMATION

Nguyen Van Thu*

Department of Physics, Hanoi Pedagogical University 2
100000, Hanoi, Vietnam

Received February 4, 2022
revised version February 4, 2022.
Accepted for publication March 18, 2022

DOI: 10.31857/S0044451022080028
EDN: Van Thu EFLSKB

The Casimir effect was first discovered [1] for the electromagnetic field confined between two neutral parallel plates at zero temperature. This effect has been studied for other fields [2–7]. In field of the Bose–Einstein condensate (BEC), the Casimir effect has been considered in both experiment [8–12] and theory, for example, [13–18] in the grand canonical ensemble and [17, 19] in the canonical ensemble. In these papers, the Casimir effect was investigated in the one-loop approximation within the framework of perturbative theory for a single dilute BEC. For two-component BEC (BECs), our previous work [20] pointed out that the Casimir force is not a simple superposition of the one of two single component BEC because of the mutual repulsive interactions. It was also proven to be zero in some cases: (i) the inter-distance between two plates becomes large enough; (ii) both the inter- and intraspecies interactions are zero (ideal gases); and an important case (iii) the interspecies interaction is the full strong segregation. Even so, the case (iii) result is controversial because of the interpretation that the original Casimir force and interspecies interactive force are of the same order in the full strong separation. As an improvement, in Ref. [21] the Casimir effect in the BECs was studied in the improved Hartree–Fock (IHF) approximation, which based on the Cornwall–Jackiw–Tomboulis (CJT) effective action formalism [22]. In this approximation the two-loop diagrams were taken into account and the Goldstone theory is obeyed. However, the momentum integrals were calculated at the lowest-order approximation, which we call the lowest-order Hartree–Fock (LIHF) approximation. Therefore, the vanishing of the Casimir force in the limit of the full strong segregation did not change.

In this paper, the Casimir effect in the BECs at zero temperature is researched in the IHF approximation with the higher-order terms of the momentum integrals and it is called the higher-order improved Hartree–Fock (HIHF) approximation. To do so, we start from the Lagrangian density of the BECs without external field [23, 24],

$$\mathcal{L} = \sum_{j=1,2} \psi_j^* \left(-i\hbar\partial_t - \frac{\hbar^2}{2m_j}\nabla^2 \right) \psi_j - V, \qquad (1)$$

with

$$V = \sum_{j=1,2} \left(-\mu_j |\psi_j|^2 + \frac{g_{jj}}{2}|\psi_j|^4 \right) + g_{12}|\psi_1|^2|\psi_2|^2. \quad (2)$$

Here $\hbar$ is the reduced Planck constant, μ_j and m_j are the chemical potential and atomic mass of component j, respectively. The coupling constant

$$g_{jj} = 4\pi\hbar^2 a_{jj}/m_j > 0$$

represents the strength of the repulsive intraspecies interaction and

$$g_{jj'} = 2\pi\hbar^2 \left(\frac{1}{m_j} + \frac{1}{m_{j'}} \right) a_{jj'} > 0$$

is the strength of the repulsive interspecies interaction, $a_{jj'}$ being the s-wave scattering length between components j and j'. The field operator ψ_j has the expectation value ψ_{j0}, which plays the role of the order

* E-mail: nvthu@live.com

parameter. Recall that for $g_{12}^2 > g_{11}g_{22}$ the two components are immiscible and a phase-segregated BEC forms [25], and vice versa. Shifting the field operators

$$\psi_j \to \psi_{j0} + \frac{1}{\sqrt{2}}(\psi_{j1} + i\psi_{j2})$$

one can obtain the CJT effective potential in the Hartree–Fock approximation. Unfortunately, this CJT effective potential was proved violating the Goldstone theorem [26] by finding the dispersion relation from the request for vanishing of the determinant of the inverse propagators [27]. To solve this problem, the method developed in [28] is invoked. After adding the extra term in the CJT effective potential, one arrives at the IHF approximation. Minimizing the CJT effective potential with respect to the order parameter one has the gap equations

$$\begin{aligned} -1 + \phi_1^2 + K\phi_2^2 + \frac{1}{g_{11}n_{10}}\,\Sigma_2^{(1)} = 0, \\ -1 + \phi_2^2 + K\phi_1^2 + \frac{1}{g_{22}n_{20}}\,\Sigma_2^{(2)} = 0. \end{aligned} \tag{3}$$

Similarly, the Schwinger–Dyson equations can be achieved by minimizing the CJT effective potential with respect to the elements of the propagators

$$\begin{aligned} \mathcal{M}_1^2 = -1 + 3\phi_1^2 + K\phi_2^2 + \frac{1}{g_{11}n_{10}}\,\Sigma_1^{(1)}, \\ \mathcal{M}_2^2 = -1 + 3\phi_2^2 + K\phi_1^2 + \frac{1}{g_{22}n_{20}}\,\Sigma_1^{(2)}. \end{aligned} \tag{4}$$

In Eqs. (3) and (4), n_{j0} is the bulk density of the component j, $K = g_{12}/\sqrt{g_{11}g_{22}}$, $\phi_j = \psi_{j0}/\sqrt{n_{j0}}$ is the dimensionless order parameter, and $\mathcal{M}_j$ is dimensionless effective mass. The self energies are defined as

$$\begin{aligned} \Sigma_1^{(1)} &= \frac{1}{2}(g_{11}P_{11} + 3g_{11}P_{22} + g_{12}Q_{11} + g_{12}Q_{22}), \\ \Sigma_1^{(2)} &= \frac{1}{2}(g_{22}Q_{11} + 3g_{22}Q_{22} + g_{12}P_{11} + g_{12}P_{22}), \\ \Sigma_2^{(1)} &= \frac{1}{2}(3g_{11}P_{11} + g_{11}P_{22} + g_{12}Q_{11} + g_{12}Q_{22}), \\ \Sigma_2^{(2)} &= \frac{1}{2}(3g_{22}Q_{11} + g_{22}Q_{22} + g_{12}P_{11} + g_{12}P_{22}), \end{aligned} \tag{5}$$

with P_{aa}, Q_{bb} are the momentum integrals.

We now consider a binary mixture of Bose gases confined between two parallel plates, which perpendicular to the z-axis. This means that the system is confined to a parallel plate geometry with the size ℓ_x, ℓ_y and distance between the two plates of $\ell = \ell_z$, which satisfies condition $\ell_x, \ell_y \gg \ell$ as was discussed in

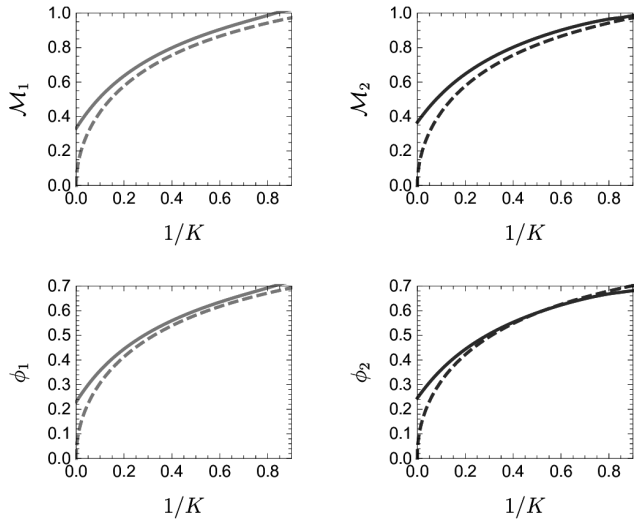

Fig. 1. (Color online) The effective masses (top panel) and order parameters (bottom panel) as a function of $1/K$ at $L = 1$. The solid red (first component) and solid blue (second component) lines are in the HIHF approximation, the dashed red (first component) and dashed blue (second component) are the corresponding quantities in the LIHF approximation

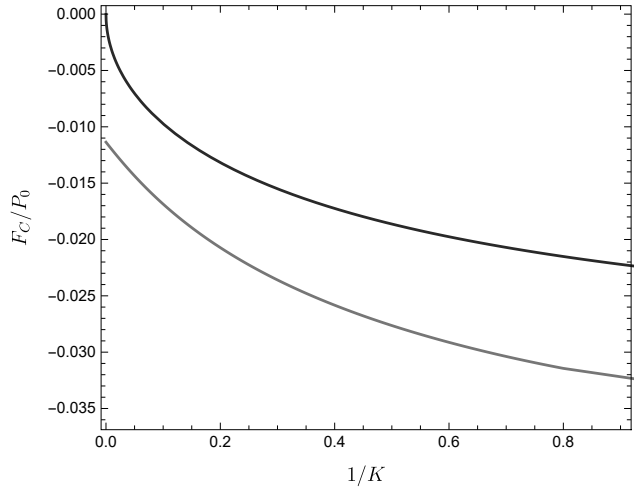

Fig. 2. (Color online) The Casimir force versus $1/K$ at $L = 1$ in the HIHF approximation (red line). The blue line corresponds to the LIHF and one-loop approximations, respectively

[29]. The periodic boundary condition is imposed at the plates, which can be realized in experiments by using toroidal traps [30,31] or optical lattices [32]. Due to the confinement, the wave vectors are quantized. Using the Euler–Maclaurin formula [33], the momentum integrals are calculated in the HIHF approximation at zero temperature

$$
\begin{aligned}
P_{11} &= -\frac{\pi^2 m_1 g_{11} n_{10} \xi_1^2}{90\hbar^2 \ell^3 \mathcal{M}_1},\\
Q_{11} &= -\frac{\pi^2 m_2 g_{22} n_{20} \xi_2^2}{90\hbar^2 \ell^3 \mathcal{M}_2},\\
P_{22} &= \frac{m_1 g_{11} n_{10} \mathcal{M}_1}{12\hbar^2 \ell} - \frac{m_1 g_{11} n_{10} \xi_1^2 \pi^2}{90\hbar^2 \mathcal{M}_1 \ell^3},\\
Q_{22} &= \frac{m_2 g_{22} n_{20} \mathcal{M}_2}{12\hbar^2 \ell} - \frac{m_2 g_{22} n_{20} \xi_2^2 \pi^2}{90\hbar^2 \mathcal{M}_2 \ell^3},
\end{aligned}
\tag{6}
$$

where $\xi_j = \hbar/\sqrt{2m_j g_{jj} n_{j0}}$ is the healing length of jth component.

In order to illustrate these calculations, numerical computations are performed for a dual-species Bose–Einstein condensates of rubidium 87 (first component) and cesium 133 (second component). For this system the parameters are in order $m_1 = 86.909u$, $a_{11} = = 100.4a_0$ for rubidium 87 and $m_2 = 132.905u$, $a_{22} = = 280a_0$ for cesium 133 [34]. Here $u = 1.66 \cdot 10^{-27}$ kg and $a_0 = 0.529$ nm are the atomic mass unit and Bohr radius, respectively. The dimensionless length is chosen as $L = \ell/\xi_1$ with $\xi_1 = 4000$ nm being the healing length of rubidium 87. The numerical computations show a significant difference compared with the corresponding result in the LIHF approximation, that is the effective masses depend on both the distance ℓ and K. The comparison of the evolution of the effective masses (top panel) and order parameters (bottom panel) in the HIHF approximation (solid lines) with those in the LIHF approximation (dashed lines) is sketched in Fig. 1 at $L = 1$. A remarkable difference in regime of the strong segregated region can be observed. In this region, at a given value of $1/K$, the values of the effective masses and order parameters in the HIHF approximation are bigger than the corresponding ones in the LIHF approximation. At the full strong segregation, both the effective masses and order parameters are different from zero whereas they vanish in the LIHF approximation. This fact confirms that the influence of the higher-order terms in the momentum integrals is not negligible. In the regime of the full strong separation, the HIHF approximation gives

$$
\begin{aligned}
\mathcal{M}_j &\simeq \frac{\mathcal{M}_{j0}}{\ell},\\
\phi_j &\simeq \frac{\phi_{j0}}{\ell^2},
\end{aligned}
\tag{7}
$$

in which

$$
\begin{aligned}
\mathcal{M}_{j0} &= \left(\frac{m_j g_{jj} \xi_j^2 \pi^2}{45\hbar^2}\right)^{1/3},\\
\phi_{j0} &= \frac{12\sqrt[3]{5}\pi^{4/3} g_{jj}^{2/3} m_j^{2/3} \xi_j^{4/3} \hbar^{4/3} - (15\pi)^{2/3} g_{jj}^{4/3} m_j^{4/3} \xi_j^{2/3}}{360\sqrt[3]{3}\hbar^{8/3}}.
\end{aligned}
\tag{8}
$$

Formally resemble the momentum integrals, the Casimir force energy density is found

$$
\mathcal{E}_C = \sum_{j=1,2} -\frac{\pi^2 m_j g_{jj} \xi_j^2 \mathcal{M}_j}{360\hbar^2 \ell^3}. \tag{9}
$$

It is clear that the Casimir energy is negative and, neglecting the ℓ-dependence of $\mathcal{M}_j$, it has the same form as the one in the LIHF approximation and one-loop approximation. However, in the LIHF and one-loop approximations, the effective masses are independent of the distance so that the Casimir energy density will be the same as the one in the one-loop approximation. The Casimir force is defined as the negative derivative of the Casimir energy with respect to a change in the distance between two parallel plates. Combining with (9) one obtains the Casimir force acting on per unit area of the plates

$$
\begin{aligned}
F_C &= \\
&= \sum_{j=1,2} \left(-\frac{\pi^2 m_j g_{jj} \xi_j^2 \mathcal{M}_j}{120\hbar^2 \ell^4} + \frac{\pi^2 m_j g_{jj} \xi_j^2}{360\hbar^2 \ell^3} \frac{\partial \mathcal{M}_j}{\partial \ell}\right).
\end{aligned}
\tag{10}
$$

Owing to the ℓ-dependence of the effective masses, the contribution of the higher-order terms in the momentum integrals is shown by second term in right-hand side of Eq. (10). The evolution of the Casimir force versus $1/K$ is plotted in Fig. 2 at $L = 1$ and other parameters are the same as in Fig. 1. The red line is drawn in the HIHF approximation whereas the blue line corresponds to the LIHF and one-loop approximations. This figure shows that the strength of the Casimir force decreases as the interspecies interaction increases. This fact is understandable if we note that the Casimir force is attractive whereas the interspecies interaction is repulsive. The red line in Fig. 2 show that the Casimir force is non-zero in the limit of the

full strong segregation within the HIHF approximation, whereas it vanishes in the LIHF and one-loop approximations as shown by the blue line in Fig. 2. This is an interesting result in comparison with that in [20]. This result gives us the conclusion that the Casimir force is always on top of interspecies interaction and this is an important improvement on the result in our previous paper [20]. Mathematically, the Casimir force in full strong separation is

$$F_C = -\sum_{j=1,2} \frac{(m_j g_{jj} \pi^2)^{4/3}}{90.3^{2/3} 5^{1/3} \hbar^{8/3} \ell^5}. \qquad (11)$$

This equation confirms again that the Casimir force is non-zero in the full strong separation limit.

Acknowledgments. We are grateful to Shyamal Biswas for their useful discussions.

Funding. This work is funded by the Vietnam National Foundation for Science and Technology Development (NAFOSTED) under Grant No. 103.01-2018.02.

The full text of this paper is published in the English version of JETP.

REFERENCES

1. H. B. G. Casimir, Proc. K. Ned. Akad. Wet. **51**, 793 (1948).

2. F. Chen, G. L. Klimchitskaya, V. M. Mostepanenko, and U. Mohideen, Phys. Rev. B **76**, 035338 (2007).

3. G. Bimonte, Phys. Rev. A **78**, 062101 (2008).

4. J. F. Babb, Adv. Atom. Mol. Opt. Phys. **59**, 1 (2010).

5. Tran Huu Phat and Nguyen Van Thu, Int. J. Mod. Phys. A **29**, 1450078 (2014).

6. M. Bordag, U. Mohideen, and V. M. Mostepanenko, Phys. Rep. **353**, 1 (2001).

7. G. L. Klimchitskaya and U. Mohideen, Rev. Mod. Phys. **81**, 1827 (2009).

8. M. Fukuto, Y. F. Yano, and P. S. Pershan, Phys. Rev. Lett. **94**, 135702 (2005).

9. A. Ganshin, S. Scheidemantel, R. Garcia, and M. H. W. Chan, Phys. Rev. Lett. **97**, 075301 (2006).

10. D. M. Harber, J. M. Obrecht, J. M. McGuirk, and E. A. Cornell, Phys. Rev. **72**, 033610 (2005).

11. J. M. Obrecht, R. J. Wild, M. Antezza, L. P. Pitaevskii, S. Stringari, and E. A. Cornell, Phys. Rev. Lett. **98**, 063201 (2007).

12. G. L. Klimchitskaya and V. M. Mostepanenko, J. Phys. A **41**, 312002 (2008).

13. J. Schiefele and C. Henkel, J. Phys. A **42**, 045401 (2009).

14. J. O. Andersen, Rev. Mod. Phys. **76**, 599 (2004).

15. D. C. Roberts and Y. Pomeau, Phys. Rev. Lett. **95**, 145303 (2005).

16. S. Biswas, J. K. Bhattacharjee, D. Majumder, K. Saha, and N. Chakravarty, J. Phys. B **43**, 085305 (2010).

17. Nguyen Van Thu, Phys. Lett. A **382**, 1078 (2018).

18. Nguyen Van Thu and Pham The Song, Physica A **540**, 123018 (2020).

19. Nguyen Van Thu, Luong Thi Theu, and Dang Thanh Hai, JETP **130**, 321 (2020).

20. Nguyen Van Thu and Luong Thi Theu, J. Stat. Phys **168**, 1 (2017).

21. Nguyen Van Thu and Luong Thi Theu, Int. J. Mod. Phys. B **33**, 1950114 (2019).

22. J. M. Cornwall, R. Jackiw, and E. Tomboulis, Phys. Rev. D **10**, 2428 (1974).

23. L. Pitaevskii and S. Stringari, *Bose–Einstein Condensation*, Oxford University Press (2003).

24. C. J. Pethick and H. Smith, *Bose-Einstein Condensation in Dilute Gases*, Cambridge University Press (2008).

25. P. Ao and S. T. Chui, Phys. Rev. A **58**, 4836 (1998).

26. T. H. Phat, L. V. Hoa, N. T. Anh, and N. V. Long, Ann. Phys. **324**, 2074 (2009).

27. S. Floerchinger and C. Wetterich, Phys. Rev. A **79**, 013601 (2009).

28. Yu. B. Ivanov, F. Riek, and J. Knoll, Phys. Rev. D **71**, 105016 (2005).

29. R. Lipowsky, in *Random Fluctuations and Pattern Growth*, ed. by H. Stanley and N. Ostrowsky, NATO ASI Series E, Vol. **157**, Kluwer Akad. Publ., Dordrecht (1988), pp. 227–245.

30. P. D. Drummond, A. Eleftheriou, K. Huang, and K. V. Kheruntsyan, Phys. Rev. A **63**, 053602 (2001).

31. J. Brand and W. P. Reinhardt, J. Phys. B **34**, L113 (2001).

32. A. A. Shams and H. R. Glyde, Phys. Rev. B **79**, 214508 (2009).

33. G. B. Arfken and H. J. Weber, *Mathematical Methods for Physicists*, Academic, San Diego (2005).

34. D. J. McCarron, H. W. Cho, D. L. Jenkin, M. P. Koppinger, and S. L. Cornish, Phys. Rev. A **84**, 011603 (2011).